



# STUDY OF QUANTUM DOT CHARACTERISTICS AND APPLICATIONS WITH SEMICONDUCTING CARBON NANOTUBE

Dr. Ranjan Prasad

Assistant Professor, S.N.S.R.K.S. College, Saharsa, B.N.M.U. Madhepura, Bihar

## ABSTRACT

The low dimensional materials exhibit unique chemical and physical characteristics that are not present in their bulk counter parts. The confinement of electrons and holes to low dimension structures results in structural modifications of quantum-size effects. The “quantum confinement effect” enables semiconductors to have atom-like structures. It can be explained by a particle in a quantum box. Quantum dots are tunable artificial atoms that provide an ideal laboratory for exploring the physics of atoms and molecules and have many potential applications. Quantum Dots are mostly assembled from semiconductor materials. They can display fluorescence in the visible range of light when excited with UV. A specific wavelength can be generated by each class of nano size materials. This makes it possible to tune the emission by altering the quantum dot size toward a particular wavelength. In this efforts characterization of quantum dots from semi conduction materials and some of their applications have been studied.

**KEYWORDS:** Quantum-Size Effects, Quantum Dots, Semiconductor Materials

## INTRODUCTION

A semiconductor of smaller size can be used for tuning the desirable Electrical, magnetic, optical, and chemical properties [9]. The low dimensional materials exhibit unique chemical and physical characteristics that are not present in their bulk counter parts. The confinement of electrons and holes to low dimension structures results in structural modifications, such as quantum-size effects [11]. The characteristic of the quantum confinement effect in quantum dots describes the size-dependent change from a continuous to a discrete energy state in the conduction and valence bands, and the corresponding widening of the band gap. The quantum confinement effect allows the semiconductors to posses the properties of atom-like structures. It can be explained by the analysis of a particle in a quantum box. QDs are semiconductor nano crystals with unique optical, thermal, and electrical characteristics. They reveal atoms whose energy levels are discrete and the band gaps change depend on the size of the QD. Now it has been possible to form one dimensional quantum dots from high quality semiconducting carbon nano tubes [1]. Quantum dots are tunable artificial atoms that provide an ideal laboratory for exploring the physics of atoms and molecules and have many potential applications. As dots can be used to controllably confine small numbers of charge carriers, they have stimulated much interest in the quantum states of a few interacting electrons. One dimensional nano tube (NT) dots are, however, very different to the 2D semiconductor dots that have been used to study effects such as the formation of all electron (Wigner) molecules [2, 3] and electronic shell filling analogous to that observed in atoms [4]. Quantum Dots are commonly assembled from semiconductor materials such as transition metal selenides, sulfides, or tellurides . Quantum dots are nano crystals that induce unique optical properties according to their sizes at the nano scale. Quantum confinement is apparent in these particles. The energy levels become discrete because of quantum confinement.

Principally, quantum dots display fluorescence in the visible range of light when excited with UV fig. (2). As the gap between the conduction and the valence bands depends on nano particle's size, the wavelength of the light emitted is linked precisely to the size of the nano particle. This makes it possible to tune the emission by altering the quantum dot size toward a particular wavelength. size. For an emission in the visible range of light, conventional Cd based the wavelength of the quantum dot emission will be related with the size of the poly dispersity in the suspension. A particular wavelength would be generated by each class of quantum dots. Due to such properties QDs make up a very important field of research, which can lead to a wide range of applications such as biomedical imagery, screen development and other new fields. Carbon dots are small carbon nano particles of sizes smaller than 10 nm. The progression of nanotechnology is growing deep to the extent of atomic level to change the optics of research. Charged particles can be confined inside the potential well. They are trapped in a lower-potential zone surrounded by higher-potential regions. The duration of the confinement determines the impact of spatial confinement on a small scale. In the case of semiconductors' exciton properties, the length scale is determined by the exciton Bohr radius ( $a^0$ ) which varies from 2 nm to 50 nm depending on the material dielectric coefficient.

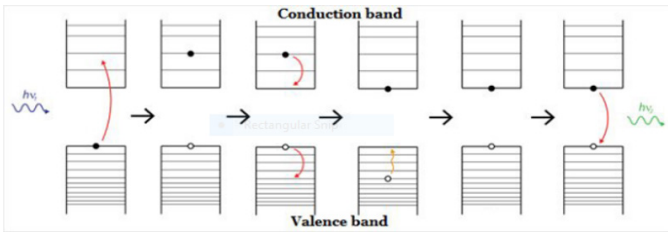


**Figure 1. Scheme of the fluorescence process in quantum dots.**

**An exciton (electron/hole pair) is formed with the UV excitation and, during its recombination, Produces light in the visible range.**

When the excited electrons leave the lower level valence band and go to the higher level conduction band they produce holes in the valence band. The hole and the displaced electron form the electro statically bounded state of electron–hole pair . It is called an exciton (Fig. 2 a). The electron-wave function is influenced by the particle's size, which is about the Bohr radius for nanostructure semi conductors. Therefore, the electron density states, energy gap, and discrete energy levels all change with respect to size (Fig. 2 b). In the bulk materials, where the band gap is smaller the electron energy levels overlap, rather than being distinct, i.e. continuous however in the nano scale materials, the band gap is larger and the individual electron energy levels appear. In the 3D universe, confinement can be in 1D, 2D, and 3D. Quantum dots and quantum wells have different physicochemical characteristics than 3D bulk solids because of the reduction in solid size, i.e., from 3D to 2D, 1 D or 0D. The zero-dimensional quantum dots (QDs) are valued for their atom-like structures.

### Model of Dot and its Analysis

Our dot model is based on the gated semiconductor NT dot device in ref. [1]. In this type of dot, the confinement potential formed in the form of electrostatic potential. The details depend on the exact specifications of the device but, near to the centre of the NT, the potential varies quadratically with a gate voltage dependent energy zero, and we use a 1D harmonic confinement potential in our model.

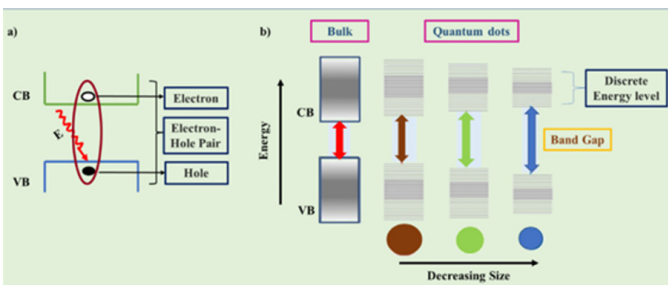


**Fig. 2. (a) Mechanism of quantum dot for generating light, and (b) Schematic illustration of quantum confinement effect: size-dependent effect shown by the QDs. As the size of the particle decreases, the distance between the valency and conduction band increases, i.e., the increase in energy band.**

Typically, the dot lengths scales are of the order of a few tens of nano meters. The dot energy scales are in the range of few meV. We consider NTs with a band gap  $E_g$  much larger than this energy scale and a unit cell length much smaller than this length scale. However, there are new features that arise from the NT band structure and these can be understood by considering the electronic structure of graphene. This type of dot can be described with an effective mass Hamiltonian.

NTs can be understood as rolled up graphene sheets and the NT states near to the conduction band minima are formed from the states of graphene near to the K and K' points. However, care must be taken when deriving the NT states because of the unusual nature of the graphene band structure near to K and K'. First, the K and K' points are equivalent, and this leads to two equivalent conduction bands in all semiconducting NTs. To derive the CNT dot states we adopt a procedure similar to refs. [14,15]. We use the two component Bloch wave functions of graphene as basis states. This gives new features into our effective mass theory for interacting electrons in a CNT quantum dot. The net result is a one dimensional 2 band effective mass Hamiltonian with a modified Coulomb interaction.

$$H = \sum_{i=1}^N \left[ \frac{-\hbar^2}{2m^*} \frac{d^2}{dz_i^2} + \frac{m^* \omega^2}{2} z_i^2 \right] + (e^2 R / 4\pi \epsilon_0 \epsilon_r) \sum_i U(z_i - z_j, R) \quad [1]$$

Here N is the number of electrons,  $\omega$  is the harmonic confinement frequency, R is the NT radius,  $\epsilon_r$  the dielectric constant. The effective mass  $m^*$  is calculated from a 4-orbital tight binding calculation with the parameterization of Porezag et al. [16]. U is the effective intra band Coulomb interaction. This effective interaction includes the effect of both the NT band structure and the cylindrical geometry of the tube. Here, we neglect the inter band Coulomb scattering because its effect on the N-particle ground state energy is small [5]. In this case the band index acts simply as an extra label by which states can be distinguished. To derive expressions for H and U we first consider the single particle NT effective mass equations starting from the Hamiltonian of a graphene sheet.

In two component form the graphene states are  $(\phi_{Ak} - e^{i\theta_k} \phi_{Bk})/\sqrt{2}$  for valence band and  $(\phi_{Ak} + e^{i\theta_k} \phi_{Bk})/\sqrt{2}$  for conduction band,  $\phi_{Ak}$  and  $\phi_{Bk}$  are the Bloch functions of the A, B sub-lattices of graphene and k is measured from the K or K' point. Then, the phase factor  $\theta_k$  is the sum of the chiral angle  $\theta$  and the polar angle  $\phi_k$  of k. In a NT k is quantized and the product of the envelope function and the Bloch function is periodic. The CNT states, written as a superposition of the Bloch states at K, are then

$$\psi(y, z) = \sum_{n\mu k_z} a_{n\mu k_z} e^{i\mathbf{k} \cdot \mathbf{r}} (\phi_{AK} + (-1)^\mu e^{i\theta_k} \phi_{BK}) / \sqrt{2}, \quad [2]$$

and there is an equivalent expression for states near K'.

**Calculation:**

To calculate the few electron states we first write  $H$  in dimensionless form by choosing the unit of energy as  $E_u = (\rho^2 m \omega^2 / \epsilon_r^2)^{1/3}$  and the unit of length as  $\lambda = [\rho / (\epsilon_r m \omega^2)]^{1/3}$ . Then, with  $x = z/\lambda$ , and dimensionless parameters,

$$\alpha^3 = [\rho^2 m^* / (\hbar^3 \epsilon_r^2 \omega)]^2 \text{ and } \beta = R/\lambda, \quad [3]$$

$$H' = \sum_{i=1}^N \left[ \frac{-1}{2\alpha} \frac{d^2}{dx_i^2} + \frac{1}{2} x_i^2 \right] + \frac{1}{2} \sum_{i \neq j} U(x_i - x_j, \beta). \quad [4]$$

$H'$  describes the interacting electron states for a parabolic dot in any NT, with any confinement frequency and any dielectric constant in terms of  $\alpha$  and  $\beta$ . Here, we consider only the region of the parameter space in which  $\hbar\omega$  and  $\epsilon_r$  take physically reasonable values

$$H = \sum_{i=1}^N \left[ \frac{-\hbar^2}{2m^*} \frac{d^2}{dz_i^2} + \frac{m^* \omega^2}{2} z_i^2 \right] \quad [5]$$

$H'$  can be diagonalised in a basis of determinantal harmonic oscillator functions to an accuracy of 0.1%. the interacting electron states for a parabolic dot in any NT, with any confinement frequency and any dielectric constant in terms of  $\alpha$  and  $\beta$  can be derived from the expression of  $H'$ .

**Results:**

By examining the electron density we identify different regimes of behaviour: in the strongly correlated regime (solid line) the Coulomb interaction dominates the single particle confinement, the electrons are pushed apart and tend to form Wigner crystal-like states with well defined peaks in the charge density for each electron. These states are similar to those studied in ref. [6] in a general 1D dot. In the 'weakly' correlated regime the interaction energy is slightly weaker than the single particle confinement energy as shown by dashed line and the electrons are forced together in the centre of the dot. There is also an intermediate regime as it is shown by dotted line. The transition between these regimes is primarily controlled by  $\alpha$  which is analogous to a mass in  $H'$ . Physically, increasing  $\alpha$  at fixed  $m^*$  and  $\epsilon_r$  corresponds to reducing the confinement  $\hbar\omega$ . If  $\alpha$  is large the electrons localise at the lowest energy minima in the potential landscape defined by the Coulomb repulsion and harmonic confinement; it is energetically favorable for the electrons to form Wigner crystal-like states. If  $\alpha$  is small however, the kinetic energy is large and the electrons can no longer localize at the Wigner lattice points. They are then confined near the centre of the dot by the harmonic potential. Here the effect of  $\beta$  is less important.

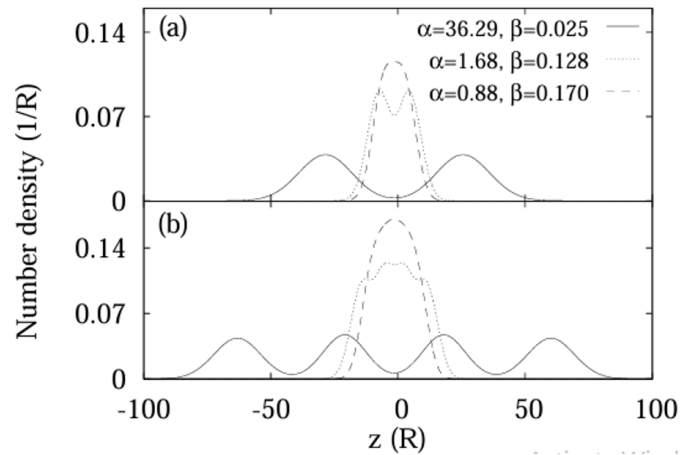


Fig. 3: Electron density for 2 (a) and 4 (b) electrons.

Reducing  $\beta$  at fixed value of  $\hbar\omega$ ,  $m^*$  and  $\epsilon_r$  corresponds to reducing  $R$ . The range of allowed  $\alpha$  depends on  $\beta$  and the different  $\alpha$  regimes are only accessible at different  $\beta$ . The physics in the different regimes of behaviour can be studied quantitatively by comparing the exact calculated 2-electron ground state energy  $E_2$  with the energies obtained with two different physical models. In the first (molecular) model we assume the electrons are strictly localised at Wigner crystal lattice sites. This approximation should be good in the strongly correlated limit where the tunneling between sites is small. In the second physical model, which should be most accurate in the weakly correlated limit, we calculate the ground state within the Hartree-Fock approximation with a harmonic oscillator single particle basis. To calculate the 2-electron ground state energy within the molecular approximation we write  $H'$  in centre of mass (CM) and relative motion (RM),  $x' = (x_1 - x_2)/\sqrt{2}$ , coordinates. The 2-electron Hamiltonian is then separable and the ground state eigenvalue of the CM part of  $H'$  is  $1/(2\sqrt{\alpha})$ . We expand the RM potential to 2nd order in  $x$  about its global minima, we see that the ground state energy increases as  $\alpha$  is reduced and the kinetic energy term in  $H'$  grows larger. We can also see that the HF method gives a poor approximation to  $E_2$ . Even in the 'weakly' correlated regime. The interaction is too strong for the HF approximation to be accurate.

**The Addition Energy:**

To make the connection to experiment we have also calculated the addition energy,  $EA(N) = E_{N+1} - 2E_N + E_{N-1}$ . Jarillo-Herrero et al [12] recently measured EA for a dot formed by gating a (35,0) semiconducting NT. They found a 2-electron periodicity in EA with oscillations of a few meV. The magnitude of the measured EA decreased smoothly with  $N$  from roughly 45 meV at  $N=1$ . When  $\alpha$  increases the oscillations in EA becomes smaller, but at large  $\alpha$  it is difficult to converge the ground state energies for  $N \geq 5$ . It is known that deformations or imperfections in the NT can split the two equivalent conduction bands [18] and, to obtain the 2-electron periodicity seen in ref. [12], we must introduce such a splitting. The different regimes of behaviour: in the strongly correlated regime (solid line) EA is featureless, oscillations begin to appear in the intermediate regime (dotted line) and become more pronounced when  $\alpha$  is

small (dashed line). We assume that the confinement potential is fixed by the design of the device and that the applied gate voltage, which controls  $N$ , alters only the energy zero of the potential. As the data in ref. [12] shows a 2-electron periodicity we focus on the 1-band results, we assume a relatively large  $\delta$  introduced by some imperfection or deformation [18] of the particular NT studied in ref. [12].

## CONCLUSION

A modified effective mass theory have been deduced of the interacting electron states in semiconducting NT dots, and exact diagonalisation calculations have been adopted to examine the effects of the interacting system in detail. In this study we have shown that correlation effects are important for almost all physically reasonable semiconducting NT dots. Our calculated addition energies for  $N < 6$  are qualitatively similar to experiment and, by investigating the 2-electron states in detail we find evidence of Wigner crystallisation in a large portion of the parameter space. NT dot devices operated in this regime would be ideal systems in which to observe quasi-1D Wigner molecules.

## REFERENCES

1. N.R. Jana, Design and development of quantum dots and other nano particles based cellular imaging probe, *Phys. Chem. Chem. Phys.* 13 (2) (2011) 385–396.
2. A.P.J.s. Alivisatos, Semiconductor clusters, nanocrystals, and quantum dots, *Science* 271 (5251) (1996) 933–937.
3. C.-H. Chuang, et al., Charge separation and recombination in CdTe/CdSe core/ shell nano crystals as a function of shell coverage: probing the onset of the quasi type-II regime, *J. Phys. Chem. Lett.* 1 (17) (2010) 2530–2535.
4. C.-H. Chuang, et al., Measuring electron and hole transfer in core/shell nanoheterostructures, *ACS Nano* 5 (7) (2011) 6016–6024.
5. M. South, S. Ozonoff, W.M. McMahon, Repetitive behavior profiles in asperger syndrome and high-functioning autism, *J. Autism Dev. Disord.* 35 (2) (2005) 145–158.
6. S. Emami, et al., Recent advances in improving oral drug bioavailability by cocrystals, *Bioimpacts: BI* 8 (4) (2018) 305.
7. L. Yue, et al., Red-emissive ruthenium-containing carbon dots for bioimaging and photodynamic cancer therapy, *ACS Appl. Nano Mater.* 3 (1) (2020) 869–876.
8. T. Ozel, G.R. Bourret, C.A.J.N.n. Mirkin, Coaxial lithography, *Nat. Nanotechnol.* 10 (4) (2015) 319–324. [9] Q. Tang, Z. Zhou, Z. Chen, Graphene-related nanomaterials: tuning properties by functionalization, *Nanoscale* 5 (11) (2013) 4541–4583.
9. M.H. Magnusson, et al., Semiconductor nanostructures enabled by aerosol technology, *Front. Phys.* 9 (3) (2014) 398–418.
10. M.-L. Chen, et al., Quantum dots conjugated with Fe<sub>3</sub>O<sub>4</sub>-filled carbon nanotubes for cancer-targeted imaging and magnetically guided drug delivery, *Langmuir* 28 (47) (2012) 16469–16476.
11. Y. Liu, et al., Upconversion nano-photosensitizer targeting into mitochondria for cancer apoptosis induction and cyt c fluorescence monitoring, *Nano Res.* 9 (11) (2016) 3257–3266.
12. Jarillo-Herrero P., Sapmaz S., Dekker C., Kouwenhoven L. P. and van der Zant H. S. J., *Nature*, 429 (2004) 389.
13. Roy M. and Maksym P. A., *Phys. Stat. Sol. (c)*, 3 (2006) 3959.
14. DiVincenzo D. P. and Mele E. J., *Phys. Rev. B*, 29 (2984) 1685.
15. Ando T., *J. Phys. Soc. Japan*, 74 (2005) 777.
16. Porezag D., Frauenheim T., Köhler T. H., Seifert G. and Kaschner R., *Phys. Rev. B*, 51 (1995) 12947.
17. E5 is accurate to  $\approx 1\%$  with  $> 3.5 \times 10^5$  Slater determinants in the expansion.
18. Ke S. H., Baranger H. U. and Yang W., *Phys. Rev. Lett.*, 91 (2003) 116803.